

An Adiabatic Quantum Electron Pump

M. Switkes^{*}, C. M. Marcus^{*}, K. Campman[†], A. C. Gossard[†]

^{*}Department of Physics, Stanford University, Stanford CA 94305

[†]Materials Department, University of California, Santa Barbara, CA 93106

A quantum pumping mechanism which produces dc current or voltage in response to a cyclic deformation of the confining potential in an open quantum dot is reported. The voltage produced at zero current bias is sinusoidal in the phase difference between the two ac voltages deforming the potential and shows random fluctuations in amplitude and direction with small changes in external parameters such as magnetic field. The amplitude of the pumping response increases linearly with the frequency of the deformation. Dependencies of pumping on the strength of the deformations, temperature, and breaking of time-reversal symmetry are also investigated.

Over the past decade, research into the electrical transport properties of mesoscopic systems has provided insight into the quantum mechanics of interacting electrons, the link between quantum mechanics and classical chaos, and the decoherence responsible for the transition from quantum to classical physics [1, 2]. The majority of this research has focused on transport driven directly by an externally applied bias. We present measurements of an adiabatic quantum electron pump, exploring a class of transport in which the flow of electrons is driven by cyclic changes in the wave function of a mesoscopic system.

A deformation of the confining potential of a mesoscopic system that is slow compared to the relevant energy relaxation times changes the wave function of the system while maintaining an equilibrium distribution of electron energies. In systems connected to bulk electron reservoirs by open leads supporting one or more transverse quantum modes, the wave function extends into the leads and these adiabatic changes can transport charge to or from the reservoirs. A periodic deformation that depends on a single parameter cannot result in net transport; any charge that flows during the first half period will flow back during the second. On the other hand, deforma-

tions that depend on two or more parameters changing in a cyclic fashion can break this symmetry and in general can provide net transport. This transport mechanism was originally described by Thouless [3] for isolated (or otherwise gapped) systems at zero temperature. The theory has recently been extended to open systems at finite temperature [4–6]. Here, we present the first experimental investigation of this phenomenon.

Before characterizing the adiabatic quantum pump in the present experiment, it is useful to recall other mechanisms that produce a dc response to an ac driving signal in coherent electronic systems. One mechanism relies on absorption of radiation to create a non-equilibrium distribution of electron energies, leading to photon-assisted tunneling [7] in systems with asymmetric tunneling leads, and a mesoscopic photovoltaic effect [9] in open systems. A second mechanism, the classical analog of the quantum pumping measured in this experiment, has been observed in single [11] and multiple [13] quantum dots in which transport is dominated by the Coulomb blockade [2]. In this regime, the capacitive energy needed to add a single electron to the system is greater than the temperature and applied bias, blockading transport through the dot. Electrons can be added one by

one by changing the potential of the isolated dot relative to the reservoirs. Each cycle begins by isolating the system from one electron reservoir—for example by increasing the height of one tunneling barrier—while forcing one or more electrons to enter from the other reservoir by changing the potential in the system. The cycle continues, reversing the configuration to isolate the system from the reservoir that supplied the electrons, and forcing the extra electrons out into the other reservoir, yielding a net flow quantized in units of the electron charge times the frequency applied. This cycle requires two ac control voltages with a phase difference between them. The magnitude and direction of the pumping are determined by these voltages; there are no random fluctuations due to quantum effects. The control and quantization of current provided by the Coulomb blockade pump has motivated its development for use as a precision current standard (see for example [14]).

Adiabatic quantum pumping in open structures also requires two ac voltages, and produces a response that is linear in the ac frequency. However, because the system is open to the reservoirs, Coulomb blockade is absent and the pumping response is not quantized. Quantum pumping is driven not by cyclic changes to barriers and potentials, but by shape changes in the confining potential or other parameters that affect the interference pattern of the coherent electrons in the device.

Many aspects of adiabatic quantum pumping can be understood in terms of emissivity, dn/dX , which characterizes the number of electrons n entering or leaving the device in response to a small change in some parameter δX , such as a distortion of the confining potential [15]. The change in the charge of the dot is thus $\delta Q = e \sum \delta X_i dn/dX_i$. Integrating the total emissivity along the closed path in the space of parameters X_i defined by the pumping cycle then yields the total charge pumped during each cycle [6]. For the particular case of pumping with two parameters (for example, shape distortions at two locations on the dot), the line integral can be written as an integral over the surface enclosed by the path, $Q \propto \int_{\alpha} \xi dX_1 dX_2$ [6] where ξ depends on the emissivities at points in parameter space enclosed by the path. Because changes in external param-

eters rearrange the electron interference pattern in the device, emissivities fluctuate randomly as parameters are changed, similar to the well-known mesoscopic fluctuations of conductance in coherent samples. When the pumping parameters make an excursion smaller than the correlation length of the fluctuations of emissivity, ξ remains essentially constant throughout the pumping cycle and the total charge pumped per cycle depends only on the area enclosed by the path in parameter space, α . These straightforward observations explain many of the qualitative features of our data.

Measurements of adiabatic quantum pumping in three similar semiconductor quantum dots defined by electrostatic gates patterned on the surface of a GaAs/AlGaAs heterostructure using standard electron-beam lithography techniques are reported. Negative voltages (~ -1 V) applied to the gates form the dot by depleting the two dimensional electron gas at the heterointerface 56 nm (device 1) or 80 nm (devices 2 and 3) below the surface. All three dots have lithographic areas $a_{\text{dot}} \sim 0.5 \mu\text{m}^2$ giving an average single particle level spacing $\Delta = 2\pi\hbar^2/m^*a_{\text{dot}} \sim 13 \mu\text{V}$ (≈ 150 mK). The three devices show similar behavior, and most of the data presented here are for device 3. In the micrograph of device 1 (Fig. 1C), the three gates marked with red circles control the conductances of the point-contact leads connecting the dot to electronic reservoirs. Voltages on these gates are adjusted so that each lead transmits $N \sim 2$ transverse modes, giving an average conductance through the dot $g \sim 2e^2/h$. The remaining two gates are used to create both periodic shape distortions necessary for pumping and static shape distortions that allow ensemble averaging [16, 19].

Except where noted, measurements were made at a pumping frequency $f = 10$ MHz, base temperature $T = 330$ mK, dot conductance $g \sim 2e^2/h \approx (13 \text{ k}\Omega)^{-1}$, and ac gate voltage $A_{\text{ac}} = 80$ mV peak-to-peak. For comparison, the gate voltage necessary to change the electron number in the dot by one is ~ 5 mV. Measurements were carried out over a range of magnetic field from 30 to 80 mT, which allows several quanta of magnetic flux, $\varphi_0 = h/e$, to penetrate the dot ($\varphi_0/a_{\text{dot}} \sim 10$ mT) while keeping the classical cyclotron radius much larger than the dot size

$(r_{\text{cyc}}[\mu\text{m}] \sim 80/B[\text{mT}])$.

The general character of quantum pumping, including antisymmetry about phase difference $\phi = \pi$, sinusoidal dependence on ϕ (for small amplitude pumping), and random fluctuations of amplitude as a function of perpendicular magnetic field is illustrated in Fig. 1. The pumping amplitude is quantified by the values A_0 and B_0 which are extracted from fits of the form $V_{\text{dot}}(\phi) = A_0 \sin \phi + B_0$ (shown as dotted lines in Fig. 1B).

As pumping fluctuations extend on both sides of zero and pumping occurs in either direction with equal likelihood for a given ϕ , $\langle A_0 \rangle$ is small and the pumping amplitude is instead characterized by $\sigma(A_0)$, the standard deviation of A_0 . For example, the data in Fig. 2B yield $\langle A_0 \rangle = 0.01 \mu\text{V}$ while the standard deviation $\sigma(A_0) = 0.4 \mu\text{V}$. Values of $\sigma(A_0)$ (Figs. 2, 3, and 4) are based on 96 independent configurations over B , V_{g1} , and V_{g2} , (Fig. 2B).

The dependence of the pumping amplitude $\sigma(A_0)$ on pumping frequency is linear (Fig. 2). For the above parameters, the linear dependence has a slope of 40 nV/MHz. As the dot has conductance $g \sim 2e^2/h$, this voltage compensates a pumped current of 3 pA/MHz, or roughly 20 electrons per pump cycle. The dependence of $\sigma(A_0)$ on the pumping strength A_{ac} (Fig. 3) shows that for weak pumping, $A_{\text{ac}} < 80 \text{ mV}$, $\sigma(A_0)$ is proportional to A_{ac}^2 , as expected from the simple loop-area argument described above. For stronger pumping $\sigma(A_0)$ increases slower than A_{ac}^2 , with a crossover from weak to strong pumping occurring at roughly the characteristic gate voltage scale of fluctuations in both dot conductance and pumping, measured independently to be $70 \pm 6 \text{ mV}$. This departure from an A_{ac}^2 dependence for strong pumping is expected to occur when the loop in parameter space describing pumping becomes sufficiently large that it encloses uncorrelated emissivities [5, 6]. In this case, one would expect $\sigma(A_0) \propto A_{\text{ac}}$. However, the observed dependence at strong pumping is slower than linear, and in fact appears consistent with $\sigma(A_0) \propto A_{\text{ac}}^{1/2}$. This unexpectedly slow dependence may result if significant heating and dephasing of electrons occurs due to strong pumping. Further study is needed to investigate this.

Another characteristic of strong pumping is that $V_{\text{dot}}(\phi)$ becomes nonsinusoidal, as seen in the lower inset of Fig. 3. Notice that $V_{\text{dot}}(\phi = \pi)$ remains close to zero for all pumping strengths while $V_{\text{dot}}(\phi = 0)$ deviates from 0 at strong pumping.

The temperature dependence of $\sigma(A_0)$ for pumping strength near the crossover from weak to strong pumping, $A_{\text{ac}} = 80 \text{ mV}$ is shown in Fig. 4. At high temperatures (1–5.5 K), $\sigma(A_0)$ is described by a power law, $\sigma(A_0) = 0.2 T^{-0.9}$ (for $\sigma(A_0)$ in μV and T in K). This behavior presumably reflects the combined influence of thermal smearing, which alone is expected to yield $\sigma(A_0) \propto T^{-1/2}$, and temperature-dependent dephasing. A similar temperature dependence is found for the amplitude of conductance fluctuations in dots [20]. Below 1K, the temperature dependence begins to round off, perhaps indicating a saturation at lower temperatures. A low-temperature saturation of pumping is expected when thermal smearing becomes less than lifetime broadening [21], $k_B T < [\Gamma_{\text{esc}} + \Gamma_{\varphi}(T)]$, where $\Gamma_{\text{esc}} = N\Delta/\pi$ (N is the number of modes per lead) is the broadening due to escape through the leads, and $\Gamma_{\varphi}(T)$ is the broadening due to dephasing, $\Gamma_{\varphi}(T) = \hbar/\tau_{\varphi}$. Using $N \sim 2$ and known dephasing times τ_{φ} in similar dots [20] yields an expected saturation at $\sim 100 \text{ mK}$, consistent with the rounding seen in the data.

Finally, we investigate the symmetries and statistical properties of adiabatic quantum pumping. The symmetry of pumping fluctuations about zero magnetic field is seen in the gray-scale plot of $V_{\text{dot}}(\phi = \pi/2)$ as a function of B and the dc voltage on one shape-distorting gate, V_{g1} (Fig. 5A). The full symmetry of pumping follows from time-reversal symmetry: $V_{\text{dot}}(\phi, B) = -V_{\text{dot}}(-\phi, -B)$, analogous to the Landauer-Büttiker relations for conductance [5]. The reduced symmetry observed in Fig. 5A, $V_{\text{dot}}(\phi, B) = V_{\text{dot}}(\phi, -B)$, results from a combination of time-reversal symmetry and the symmetry $V_{\text{dot}}(\phi, B) = -V_{\text{dot}}(-\phi, B)$ implied by the sinusoidal dependence of V_{dot} on ϕ at low pumping amplitudes.

A central paradigm in mesoscopic physics is that the statistical properties of a fluctuating quantity depend on symmetries of the system and little else. In order to investigate how the statistics of pumping fluctuations depend on time-reversal symmetry, we

have measured $V_{\text{dot}}(\phi = \pi/2)$, as well as the conductance, as a function of magnetic field for 36 independent configurations of V_{g1} and V_{g2} . The sampling in B is much finer than the characteristic magnetic field scales for pumping fluctuations (3.3 ± 0.4 mT) and conductance fluctuations (3.9 ± 0.4 mT), where these values are the half-maxima of the autocorrelations of the fluctuations. These values are comparable to and somewhat smaller than one flux quantum through the device, consistent with theory and previous experiments on conductance in similar dots [22]. The average pumped voltage, $\langle V_{\text{dot}}(\phi = \pi/2) \rangle$ is close to zero and has no outstanding features other than its symmetry in magnetic field. On the other hand $\sigma(V_{\text{dot}}(\phi = \pi/2))$, shows a peak at $B = 0$ of roughly twice its value away from zero field. The peak width is comparable to the correlation field (Fig. 5B), suggesting that the peak is associated with the breaking of time-reversal symmetry. We conclude that pumping fluctuations are larger for the time-reversal symmetric case at $B = 0$, similar to the situation for conductance fluctuations [16].

References

- [1] C. W. J. Beenakker and H. Van Houten, in *Solid State Physics*, H. Ehrenreich and D. Turnbull eds. (Academic Press, San Diego, 1991), vol. 44, pp. 1–228
- [2] L. P. Kouwenhoven, et al., in *Proceedings of the Advanced Study Institute on Mesoscopic Electron Transport*, L. P. Kouwenhoven, G. Schön, L. L. Sohn eds. (Kluwer, Dordrecht, 1997), Series E
- [3] D. J. Thouless, *Phys. Rev. B* **27**, 6083 (1983)
- [4] B. Spivak, F. Zhou, M. T. Beal Monod, *Phys. Rev. B* **51**, 13226 (1995)
- [5] F. Zhou, B. Spivak, B. L. Altshuler, *Phys. Rev. Lett.* **82**, 608 (1999)
- [6] P. W. Brouwer, *Phys. Rev. B* **58**, 10135 (1998)
- [7] L. P. Kouwenhoven, et al., *Phys. Rev. B* **50**, 2019 (1994)
- [8] L. P. Kouwenhoven, et al., *Phys. Rev. Lett.* **73**, 3443 (1994)
- [9] V. I. Fal’ko and D. E. Khmel’nitskiĭ, *Zh. Eksp. Teor. Fiz.* **95**, 328 (1989) [*Sov. Phys. JTEP* **68**, 186 (1989)]
- [10] J. Liu, M. A. Pennington, N. Giordano, *Phys. Rev. B* **45**, 1267 (1992)
- [11] L. P. Kouwenhoven, A. T. Johnson, N. C. van der Vaart, C. J. P. M. Harmans, C. T. Foxon, *Phys. Rev. Lett.* **67**, 1626 (1991)
- [12] L. P. Kouwenhoven, et al., *Z. Phys. B* **85**, 381 (1991)
- [13] H. Pothier, P. Lafarge, C. Urbina, D. Esteve, M. H. Devoret, *Europhys. Lett.* **17**, 249 (1992)
- [14] M. W. Keller, J. M. Martinis, R. L. Kautz, *Phys. Rev. Lett.* **80**, 4530 (1998)
- [15] M. Büttiker, H. Thomas, A. Prêtre, *Z. Phys. B* **94**, 133 (1994)
- [16] H. U. Baranger and P. A. Mello, *Phys. Rev. Lett.* **73**, 142 (1994)
- [17] R. A. Jalabert, J.-L. Pichard, C. W. J. Beenakker, *Europhys. Lett.* **27**, 255 (1994)
- [18] I. H. Chan, R. M. Clarke, C. M. Marcus, K. Campman, A. C. Gossard, *Phys. Rev. Lett.* **74**, 3876 (1995)
- [19] Voltages on these gates have a dc component, V_g , and an ac component (at MHz frequencies) produced using two frequency-locked synthesizers (HP 3325) with a computer-controlled phase difference ϕ between them. To allow a sensitive lock-in measurement of the pumping signal, the ac gate voltages are chopped by a low-frequency (93 Hz) square wave, and the voltage across the dot measured synchronously using a PAR 124 lock-in amplifier. A bias current can also be applied directly from the lock-in amplifier allowing conductance to be measured without disturbing the measurement set-up. The current bias is then set to zero to measure pumping

- [20] A. G. Huibers, M. Switkes, C. M. Marcus, K. Campman, A. C. Gossard, *Phys. Rev. Lett.* **81**, 1917 (1998)
- [21] F. Zhou, personal communication (1998)
- [22] C. M. Marcus, et al., *Chaos, Solitons, & Fractals* **8**, 1261 (1997)
- [23] The line of symmetry is slightly shifted from the “ $B = 0$ ” line determined from the magnet current due to offset magnetic fields
- [24] We thank A. Auerbach, P. Brouwer, A. Morpurgo, B. Spivak, and F. Zhou for useful discussions. We acknowledge support at Stanford from the ARO under contract DAAH04-95-1-0331 and the NSF-PECASE under contract DMR-9629180-1, and at UCSB from the AFOSR under Grant No. F49620-94-1-0158 and by QUEST, an NSF Science and Technology Center.

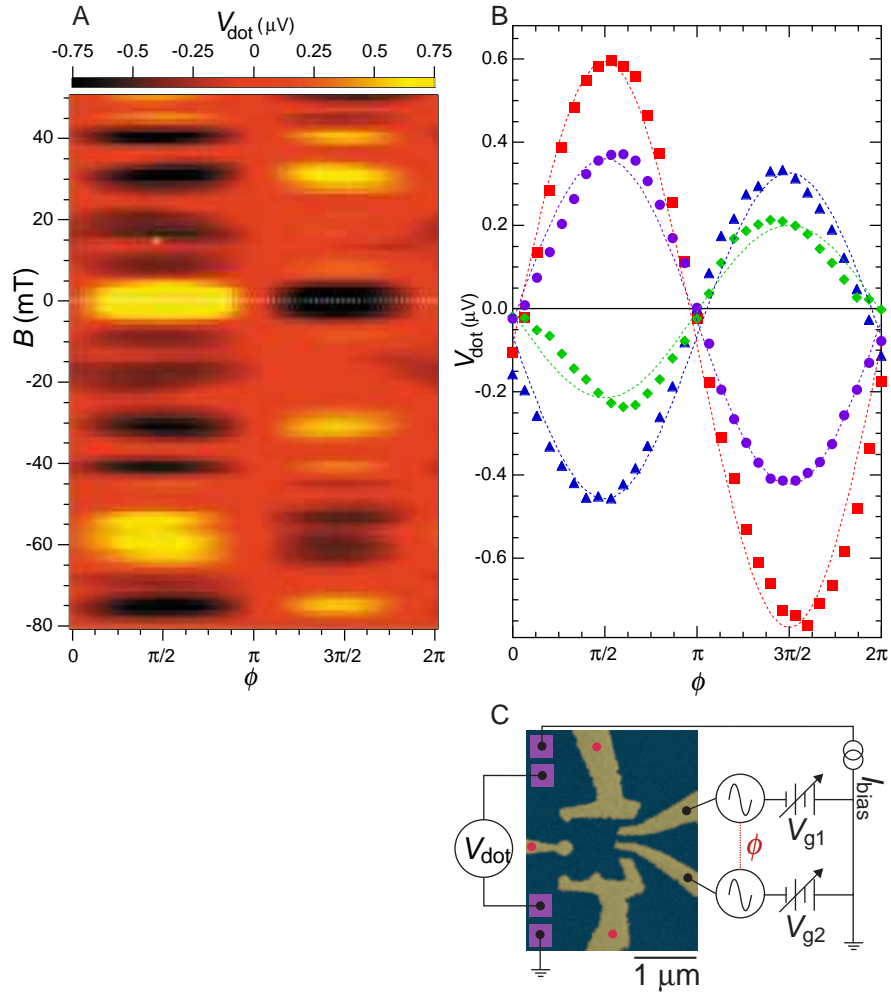


Figure 1: (A) Pumped dc voltage V_{dot} as a function of the phase difference ϕ between two shape-distorting ac voltages and magnetic field B . Note the sinusoidal dependence on ϕ and the symmetry about $B = 0$ (dashed white line). (B) $V_{\text{dot}}(\phi)$ for several different magnetic fields (solid symbols) along with fits of the form $V_{\text{dot}} = A_0 \sin \phi + B_0$ (dashed curves). (C) Schematic of the measurement setup and micrograph of device 1. I_{bias} is set to 0 for pumping measurements.

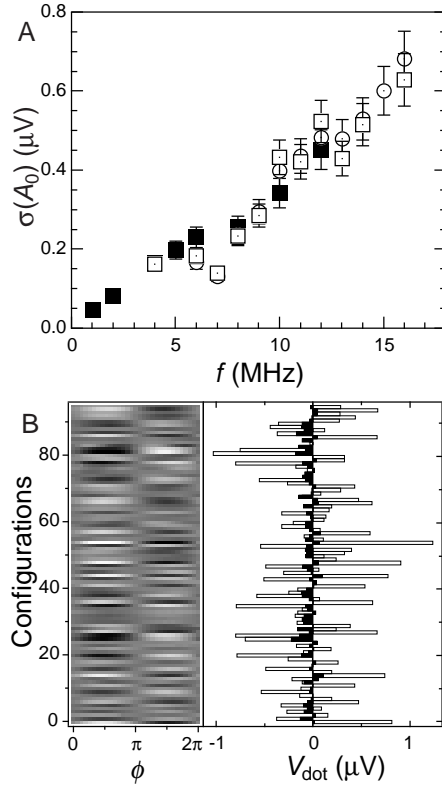


Figure 2: (A) Standard deviation of the pumping amplitude, $\sigma(A_0)$, as a function of ac pumping frequency. The slope is $\sim 40 \text{ nV/MHz}$ for both device 2 (solid symbols) and 3 (open symbols). Circular symbols represent a second set of data taken for device 3. (B) A typical data set corresponding to one point in (A), along with fit parameters A_0 (open bars) and B_0 (solid bars) for each configuration.

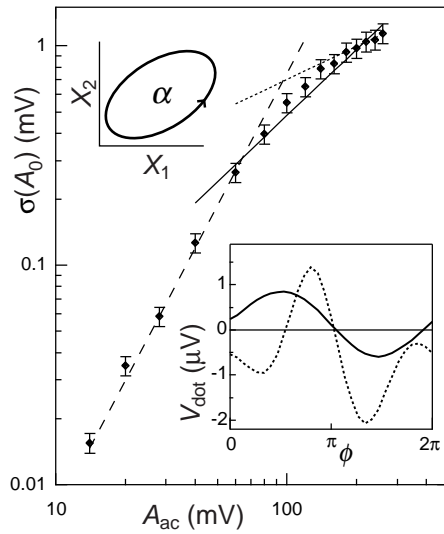


Figure 3: Standard deviation of the pumping amplitude, $\sigma(A_0)$, as a function of the ac driving amplitude A_{ac} , along with fits to $\sigma(A_0) \propto A_{ac}^2$ below 80 mV (dashed line), $\sigma(A_0) \propto A_{ac}$ (solid line), and $\sigma(A_0) \propto A_{ac}^{1/2}$ (dotted line) above 80 mV. Lower Inset: Sinusoidal dependence of $V_{dot}(\phi)$ at small and intermediate A_{ac} (solid curve, $A_{ac} = 100$ mV) becomes nonsinusoidal for strong pumping (dotted curve, $A_{ac} = 260$ mV), but maintains $V_{dot}(\pi) = 0$, required by time-reversal symmetry. Upper Inset: Schematic of the loop swept out by the pumping parameters X_1 and X_2 . The charged pumped per cycle can be written in terms of an integral over the surface α enclosed by the loop.

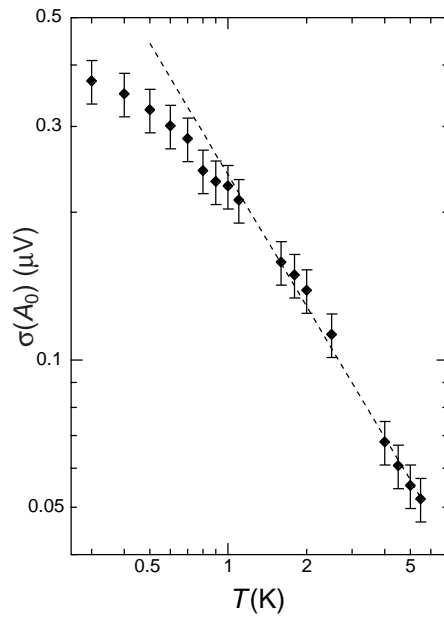


Figure 4: Pumping amplitude $\sigma(A_0)$ as a function of temperature T with a power law fit (dashed line). At lower temperatures, there is a rounding off of the T dependence, consistent with an expected saturation when lifetime broadening exceeds temperature below ~ 100 mK.

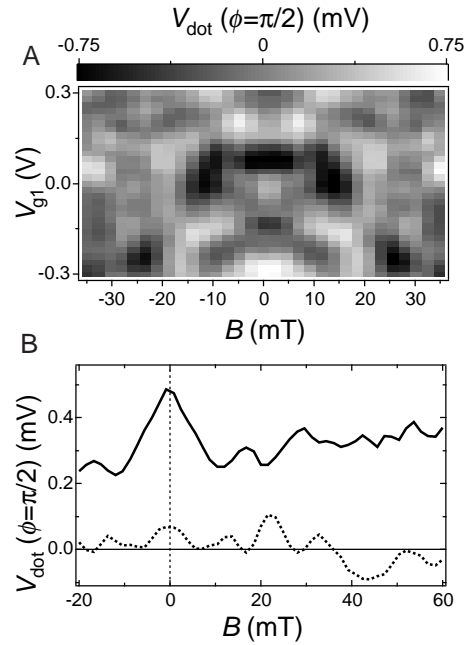


Figure 5: (A) Gray-scale plot of $V_{\text{dot}}(\phi = \pi/2)$ as a function of magnetic field B and dc gate voltage V_{g1} [23]. Note the symmetry and the characteristic scales of pumping fluctuations. (B) Average (dotted curve) and standard deviation (solid curve) of 36 uncorrelated samples of $V_{\text{dot}}(\phi = \pi/2)$ as a function of B measured at different dc gate voltages, V_{g1} and V_{g2} [not the same data set as (A)]. The average is small and fluctuates around zero. The standard deviation shows a peak around $B = 0$ roughly twice its value away from zero with a width corresponding to roughly one quantum of flux, h/e , through the dot. The reduction of pumping fluctuations away from $B = 0$ is presumably associated with the breaking of time-reversal symmetry, similar to the reduction of conductance fluctuations seen upon breaking time-reversal symmetry [16].